Laboratory Investigation

In Vivo Technetium-99m S12 Antibody Imaging of Platelet α-Granules in Rabbit Endothelial Neointimal Proliferation After Angioplasty

D. Douglas Miller, MD; Andrew J. Boulet, MD; Fermin O. Tio, MD; Oscar J. Garcia, MD; Douglas M. Guy, MD; Rodger P. McEver, MD; Julio C. Palmaz, MD; Koon Yan Pak, PhD; Donald S. Neblock, PhD; Harvey J. Berger, MD; and Peter E. Daddona, PhD

To examine the specificity of technetium-99m monoclonal antibody (S12) imaging for identifying activated platelets at interventional injury sites in atherosclerotic rabbit arteries, subgroups of unheparinized rabbits ($n=39$) underwent serial percutaneous transluminal aortic angioplasty (PTA) procedures (with or without intravascular stent placement) followed by in vivo and then ex vivo gamma camera imaging, scanning, and immunoelectron microscopy to determine the intravascular loci of S12 Fab′ antibody binding. Despite angiographic vessel patency, image-derived ratios of in vivo S12 binding in injured versus uninjured vascular segments were significantly increased ($p<0.05$) after one PTA (1.3±0.17, $n=7$), PTA twice at 6-week intervals (1.4±0.22, $n=7$), and PTA plus stent placement (1.6±0.28, $n=7$) compared with control experiments (1.1±0.13, $n=7$). Ex vivo imaging of blood-free excised aortas confirmed S12 localization at PTA (2±0.4, $n=3$) and PTA plus stent placement (5±3.8, $n=7$) sites (both $p<0.05$ versus controls). S12 antibody uptake decreased significantly ($p<0.05$) at 1 week after PTA plus stent placement in vivo (1.1±0.10, $n=4$) and ex vivo (1.6±0.7, $n=3$). Electron microscopic studies confirmed dense platelet, fibrin, and red blood cell deposition in regions of acute injury, with endothelial neointimal proliferation at 1 week after PTA. Immunoelectron microscopic studies confirmed specific in vivo S12 binding (22:1 versus nonrelevant IgG) at sites of α-granule GMP-140 expression in activated platelets. Therefore, S12 studies may be useful to localize sites of platelet-derived mitogen release at arterial PTA injury sites. (*Circulation* 1991;83:224–236)

Platelet aggregation and degranulation are frequently implicated in the pathogenesis of acute coronary syndromes such as unstable angina pectoris and myocardial infarction.[1–4] Therapy for these acute ischemic syndromes and for prevention of acute vessel closure after angioplasty includes intravenous nitroglycerin, heparin, and aspirin, all agents with significant antiplatelet effects.[4–8] However, antiplatelet and vasodilator drugs have uniformly failed to prevent early (less than 6 months) restenosis after percutaneous transluminal coronary angioplasty (PTCA).[9–15] The principal pathogenetic mechanism for premature restenosis after successful angioplasty appears to be platelet activation with release of growth factors[7,16] that cause intimal smooth muscle proliferation,[17–21] which vitiates the original PTCA improvement.

One approach to visualizing platelet activity in vascular injury sites has been radionuclide imaging of indium-111–labeled autologous platelets.[22–25] The usefulness of these studies is compromised by 1) the need to remove platelets for labeling followed by

From the Departments of Medicine and Radiology (D.D.M., A.J.B., F.O.T., O.J.G., D.M.G., J.C.P.), University of Texas Health Science Center at San Antonio, Tex., Centocor, Inc. (K.Y.P., D.S.N., H.J.B., P.E.D.), Department of Immunobiology, Research and Development Division, Malvern, Pa., and St. Francis Medical Research Institute and Department of Medicine (R.P.M.), University of Oklahoma Health Sciences Center, Oklahoma City, and Cardiovascular Biology Research Program, Oklahoma Medical Research Foundation, Oklahoma City, Okla.

Presented in part at the 62nd Scientific Sessions of the American Heart Association, New Orleans, La., November 1989.

Supported in part by American Heart Association, Texas Affiliate, Grant-In-Aid 88G-355.

Address for reprints: D. Douglas Miller, MD, Associate Professor of Medicine, Department of Medicine/Cardiology, University of Texas Health Science Center, 7703 Floyd Curl Drive, San Antonio, TX 78284-7872.

Received March 5, 1990; revision accepted August 14, 1990.

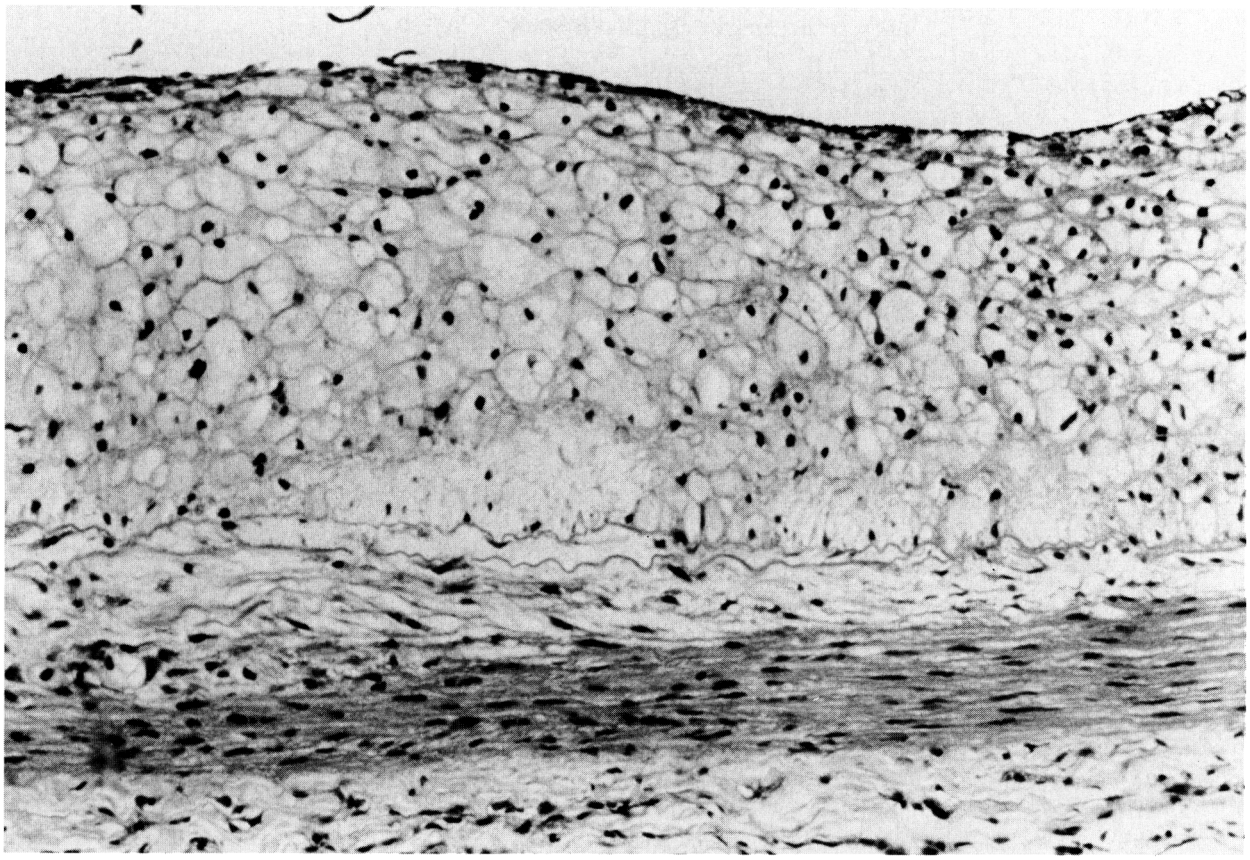

FIGURE 1. *Photomicrograph of extensive atherosclerotic changes in a rabbit aorta adjacent to site of percutaneous transluminal angioplasty plus stent placement. Intima is markedly thickened (intima-to-media ratio, 1.9±0.92) and contains numerous cholesterol-laden foamy macrophages. Endothelial cells are present covering atherosclerotic intima. Media is intact, with minimal fibromuscular components present in intima.*

reinfusion, 2) high blood pool background activity, and 3) the requirement for the thrombus to incorporate new labeled platelets at the time of the study. Infusion of radiolabeled monoclonal antibodies specific for the platelet plasma membrane glycoprotein IIb-IIIa complex has been tested in venous thrombus models[26] but remains limited by high blood pool background originating from both activated and unactivated labeled circulating platelets.

Another group of monoclonal antibodies specific for activated platelets identifies the α-granule membrane protein GMP-140, also known as PADGEM protein,[27–30] which is redistributed to the cell surface during fusion of α-granule membranes with the plasma membrane. Therefore, monoclonal antibodies to GMP-140 are specific for and bind only to the surface of stimulated platelets. Imaging studies with radiolabeled polyclonal antibodies to GMP-140 have identified venous thrombi in a baboon model.[31]

This study was performed to evaluate technetium-99m–labeled S12, a monoclonal antibody to GMP-140,[27,28] for imaging intravascular platelet-rich thrombi in a graded arterial injury rabbit model. In vivo imaging was correlated with ex vivo imaging, scanning, and immunoelectron microscopic pathological analysis to determine the specificity and loci of antibody uptake.

Methods

Animal Model

The S12-subtype Fab′ fragment is cross-reactive with human, nonhuman primate (i.e., baboon), and rabbit platelets but has poor affinity for canine and porcine platelets. Therefore, two rabbit models were developed for these studies.

Adult male New Zealand White rabbits (n=39) weighing 5–10 lb (3–5 kg) were studied according to a protocol approved by the Institutional Animal Care and Use Committee (IACUC) of the University of Texas Health Science Center at San Antonio. All surgical procedures were performed according to IACUC and AAALAC guidelines by experienced operators. Excluding controls fed standard rabbit chow (n=7), all animals were placed on an atherogenic diet consisting of commercially available rabbit pellets (ICN Biochemicals, Cleveland, Ohio) treated with 2% cholesterol and 6% peanut oil. A separate control group (n=7) was fed a high cholesterol diet but did not have PTA or stenting performed. After a minimum of 2 weeks of feeding, serum cholesterol

TABLE 1. S-12 Monoclonal Antibody Arterial Injury Ratios

Study group	*n*	In vivo	*n*	Ex vivo
Unfed controls	7	1.09±0.13	4	0.96±0.11
Cholesterol-fed controls	7	1.18±0.13	4	1.27±0.52
PTA×1	7	1.31±0.17*	3	2.06±0.35*‡
PTA×2 (6 wk)	7	† 1.43±0.22*	2	† 3.5
PTA+stent	7	1.57±0.28*‡	7	5.3±3.8*‡
PTA+stent (1 wk)	4	† 1.12±0.10	3	† 1.6±0.69
Carotid TEC	4	1.23±0.06	2	4.8

PTA, percutaneous transluminal angioplasty; TEC, transluminal extraction catheter atherectomy.
*$p<0.05$ versus unfed controls.
†$p<0.05$ between study groups.
‡$p<0.05$ versus cholesterol-fed controls.

levels were significantly elevated in fed animals compared with those of unfed controls (1,277±873 versus 117±91 mg/dl, $p<0.01$).

Animals were sedated with an intramuscular mixture of ketamine (100 mg/ml, 9-ml aliquot; Fort Dodge, Fort Dodge, Iowa), xylazine (100 mg/ml, 0.36-ml aliquot; Haver-Mobay, Shawnee, Kan.), and chlorpromazine (25 mg/ml, 3-ml aliquot; Goldine, Miami, Fla.). Using the Baumgartner technique of atherogenesis,[32] balloon endothelial denudation injury of the infrarenal aorta was followed by feeding for a minimum of 4–6 weeks using the atherogenic diet to enhance insudation of cholesterol into the injured arterial segments. This model produced significant atherosclerotic lesions, as shown in Figure 1.[33–35]

Giant Flemish rabbits ($n=4$), weighing 15–20 lb (7–10 kg), were used for transluminal extraction catheter (TEC) atherectomy of the carotid arteries. The Baumgartner technique was used to produce typical arteriosclerotic lesions in the midportion of both internal carotid arteries, after which one artery underwent TEC atherectomy, and the other served as the control artery. Other than heparin use in TEC studies, animals were not treated with platelet-inhibiting medications before these or subsequent interventional injury procedures.

Interventional Procedures

Percutaneous transluminal angioplasty. PTA was performed once in seven animals and twice at 6-week intervals in seven rabbits. PTA was performed by either retrograde cannulation of the infrarenal aorta through a contralateral femoral arteriotomy or by selective cannulation of the artery using an over-the-wire technique. Standard 3.0–3.5-mm-diameter angioplasty balloon catheters were used (USCI, Billerica, Mass.). After fluoroscopic localization (L_{1-2} vertebral level), the balloon was hand-inflated to 3–4 atm to overdilate the artery. An abdominal aortogram was obtained by serial filming after injection of 3–4 ml of 43% diatrizoate meglumine contrast medium over 1 second.

Intravascular stent placement. PTA and stent placement were performed in 11 rabbits,[24–26] seven of which were studied acutely, and four of which were examined 1 week later. Balloon-expandable intraluminal grafts, or "stents" (Johnson and Johnson Co., Warren, N.J.), were delivered using a left carotid arteriotomy incision. A 5F introducer sheath with check valve and side-arm (Cordis, Miami, Fla.) was fluoroscopically directed toward the descending aorta. A stent of 1.7-mm i.d. (unexpanded)×15-mm length was coaxially mounted on the angioplasty balloon for delivery over a 0.014-in. wire to the infrarenal aorta (L_{1-2} vertebral level). The angioplasty balloon was fully expanded to place the stent and then deflated and withdrawn. An abdominal aortogram confirmed stent position, expansion, and patency.

Transluminal extraction catheter atherectomy. TEC atherectomy procedures were performed in four rabbits through a femoral arteriotomy incision using a flexible angioplasty guide wire that was fluoroscopically advanced into the right carotid artery. Several integrade passes were made with the TEC along the length of the carotid artery. Contrast angiography of both carotid arteries was performed before and after atherectomy.

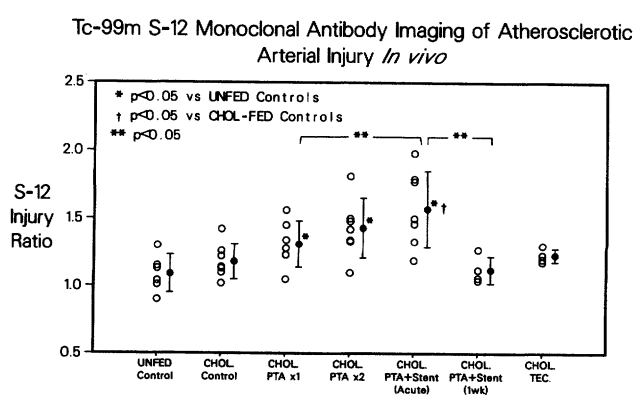

FIGURE 2. *Scatterplot of in vivo S12 injury ratios in all rabbit subgroups* (n=43). *Mean±1 SD for each subgroup is given. There was a progressive increase in S12 uptake in aortic segments of exposed to repeated or more aggressive acute injury. This increase was not observed in studies 1 week after percutaneous transluminal angioplasty (PTA) heparinized transluminal extraction catheter (TEC) studies.*

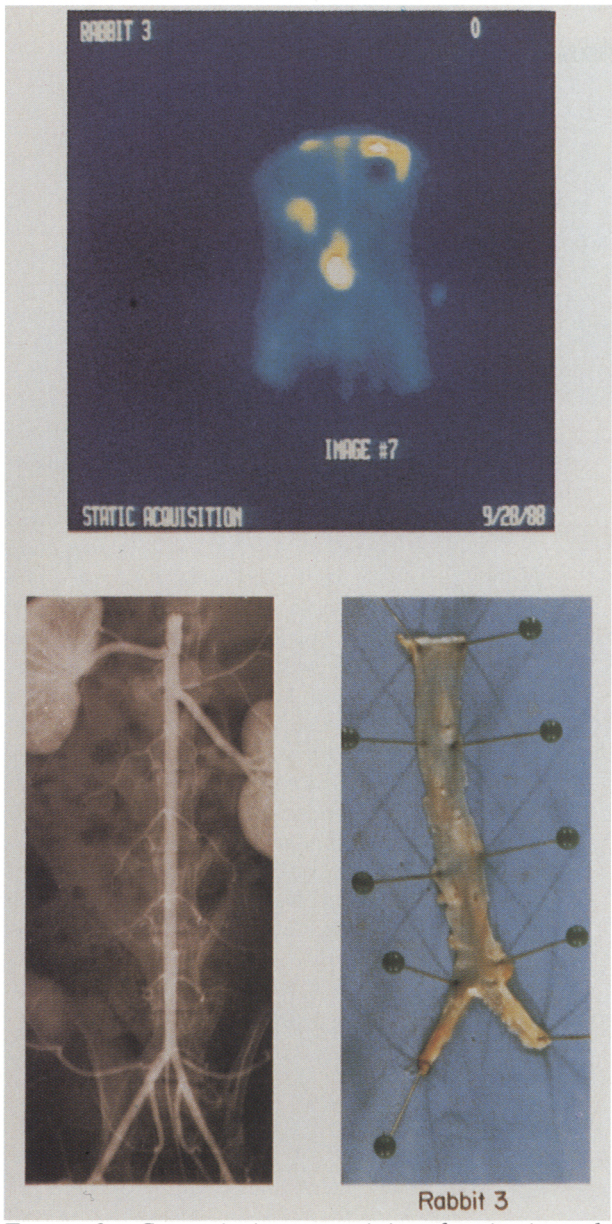

FIGURE 3. *Composite image consisting of an in vivo technetium-99m S12 antibody image* (upper panel), *contrast aortogram* (lower left panel), *and gross pathology* (lower right panel) *from a cholesterol-fed control rabbit. Aorta is angiographically patent, with minimal pathological evidence of fatty streaks at origin of vertebral arteries. In vivo S12 antibody image demonstrates absence of focal uptake in infrarenal aorta, with intense uptake in the bladder and in the lower pole of the left kidney (partially shielded) 1 hour after injection.*

Technetium-99m S12 Fab' Antibody Radionuclide Imaging

The S12 Fab′ antibody fragment was prepared from hybridoma-produced IgG and labeled with ^{99m}Tc using the two-vial kit method of Pak et al.[36] The final specific activity was 20 mCi ^{99m}Tc/mg S12 protein. The incorporation of ^{99m}Tc was quantitated by gel-filtration high-performance liquid chromatography equipped with a radiometric detector and instant thin-layer chromatography (Gelman Sciences). Preparations with labeling efficiency of less than 90% were discarded.

Planar anterior–view gamma camera images were acquired using a large field-of-view camera (MEDX 37, Searle) peaked to the 140-kev major energy photopeak of ^{99m}Tc (10% window) and a high-resolution parallel hole collimator. Serial studies were acquired every 5 minutes for 1 hour beginning 20 minutes after the ear vein injection of 5 mCi/0.4 mg (400 μg) of ^{99m}Tc-labeled S12 antibody injected within 15 minutes of injury. Appropriate shielding of the secondary uptake in background organs, including bladder, kidneys, salivary glands, and thyroid glands, was performed as needed to optimize vascular target counts. In vivo images of the aorta (versus psoas muscle) and carotid (versus sternocleidomastoid muscle) arteries 1 hour after injection had target-to-background ratios averaging 2.9±0.9.

A total of more than 400,000 counts (5 minutes) was acquired in in vivo abdominal aortic scintigrams at 1 hour after injection; a total of 10,000 counts (30 minutes) was acquired in ex vivo artery images. A 10–20-μCi point source was used to define the upper and lower ends of the aorta after ex vivo imaging.

Operator-defined fixed regions-of-interest (ROIs) were assigned by a blinded experienced nuclear medicine technician to the injured areas of the infrarenal aorta and carotid artery for comparison to uninjured aortic and carotid segments. Counts per pixel in these ROIs were used to generate a ratio of counts in the injured to counts in the uninjured segments—the "injury ratio." An injury ratio of 1.5 indicates a 50% increase of local ^{99m}Tc S12 uptake compared with normal blood pool activity.

Control animals (without vascular injury) had aortic activity analyzed in vessels of comparable luminal size and anatomical location in an identical fashion to animals undergoing serial PTA and/or stent placement. Briefly, in each animal, the appropriate aortic contrast angiogram was used to assist in the placement of ROIs in the upper half and lower half of the infrarenal aorta above the iliac bifurcation. Detailed necropsy dissections were carried out to demonstrate the anatomical location of the infrarenal aorta and iliac arteries to the nuclear technician charged with placing ROIs for the calculation of the injury ratio. If in the opinion of two blinded nuclear physicians, the ROIs selected were incorrectly placed lateral to the aorta, above the renal arteries, or below the aortic bifurcation, the original ROIs were corrected by a consensus of all trained observers. Minimal midline blood pool activity was usually present 1 hour after injection to assist ROI placement. Blood pool aortic activity from earlier (0–60 minutes) images was also helpful in identifying aortic ROIs.

Pathological Studies

Animals were killed with an intravenous overdose of pentobarbital (50 mg/kg). Randomly selected aortas were excised from the level of renal arteries to 1

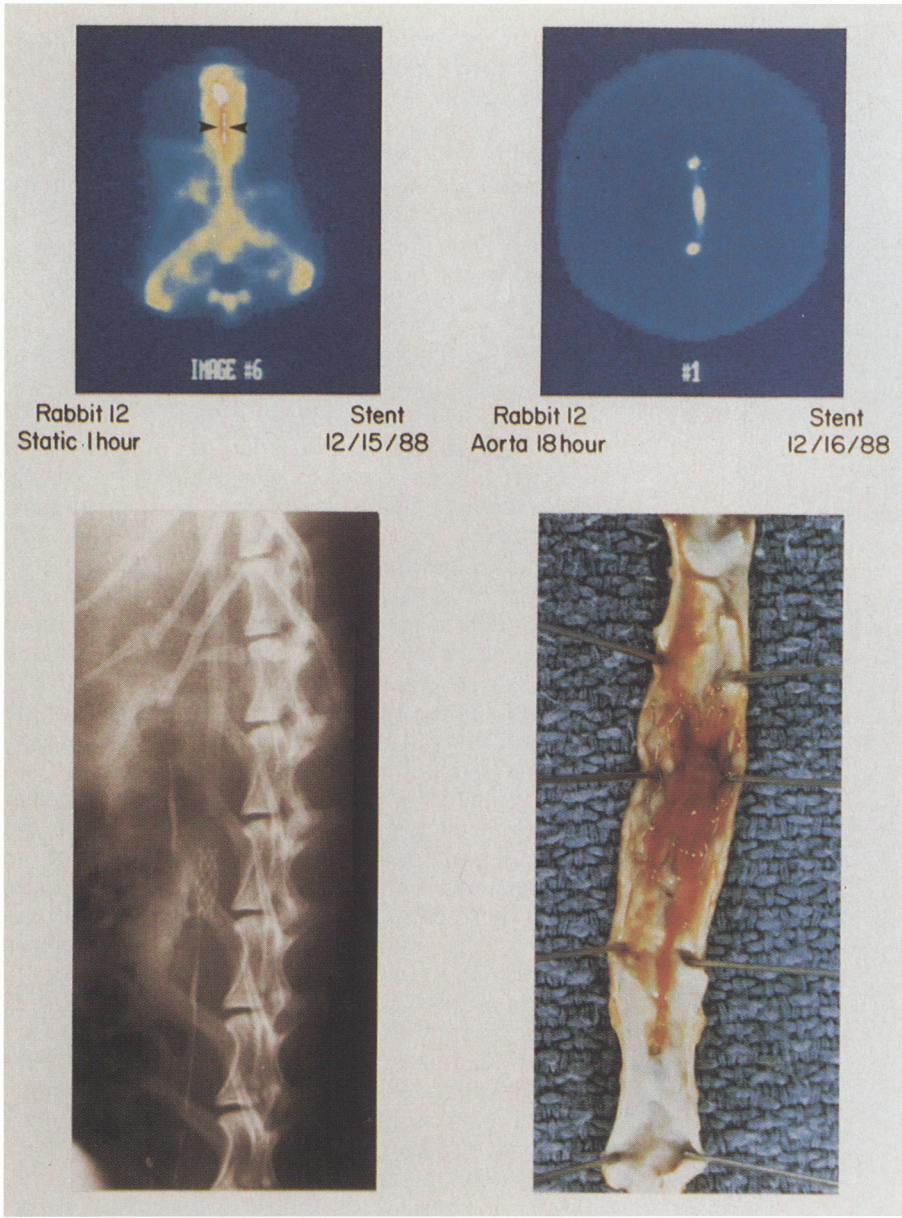

FIGURE 4. Left four panels: *This composite image comprises in vivo technetium-99m S12 antibody images acquired 1 hour after injection* (upper left) *and ex vivo after excision of the aorta 18 hours after injection* (upper right). *There is intense focal uptake of S12 antibody activity at the site of percutaneous transluminal angioplasty (PTA) plus stent placement (arrows), which is visualized in vivo and on the ex vivo excised aorta image (injury ratio, 1.8 in vivo and 2.8 ex vivo). Area of PTA plus stent placement is angiographically patent as demonstrated in the radiograph* (lower left panel) *and by contrast injection (not shown). Gross pathology* (lower right panel) *demonstrates extensive fibrin, red blood cell, and platelet thrombus adherent to the stent at area of PTA, with atherosclerotic vascular changes in uninjured aorta.* Right panel: *Enlargement of upper left in vivo imaging panel clearly demonstrates focal ^{99m}Tc S12 activity at the infrarenal PTA plus stent placement site.*

cm below the iliac bifurcation for ex vivo imaging of ^{99m}Tc S12 antibody activity. The aortas were washed free of blood by gentle plastic catheter infusion of normal saline before imaging.

Aortas not selected for ex vivo imaging underwent 0.25% silver nitrate staining and then pressure fixation in situ at 100 mm Hg for more than 12 hours with a 4% buffered formaldehyde solution. The infrarenal aorta and iliac arteries were then surgically removed for subsequent histological processing.

Specimens were initially transluminated and photographed under a microscope at low power. Sections taken from the midportion and both ends of the injured area as well as cross-sections obtained above and below the area of injury were stained with hematoxylin and eosin, trilastic, and oil red O. The other half of the injured aortic wall was postfixed in 2% osmium tetroxide and studied by scanning and transmission electron microscopy. A histomorphometric ratio of intimal to medial wall thickness was also derived from each cross section at 70 levels along the length of each vessel. Ultrathin sections of blood clots extracted from the angioplasty-injury regions of the aorta were immunostained with monoclonal S12 antibody and preimmunized rabbit anti-mouse and goat anti-rabbit IgG conjugated with 10 nm colloidal gold. The rabbit and goat sera were used as the negative control. Known positive controls for the secondary and tertiary antibodies were also carried out.

Statistical Analysis

In vivo and ex vivo imaging data are summarized in Table 1 and are presented as the mean group values ±1 SD. After the performance of a Wilk-Shapiro test of normality, the mean values (±1 SD) of parametric and nonparametric data for continuous pathology and image-derived parameters were statistically compared using a two-tailed *t* test. A significance level of

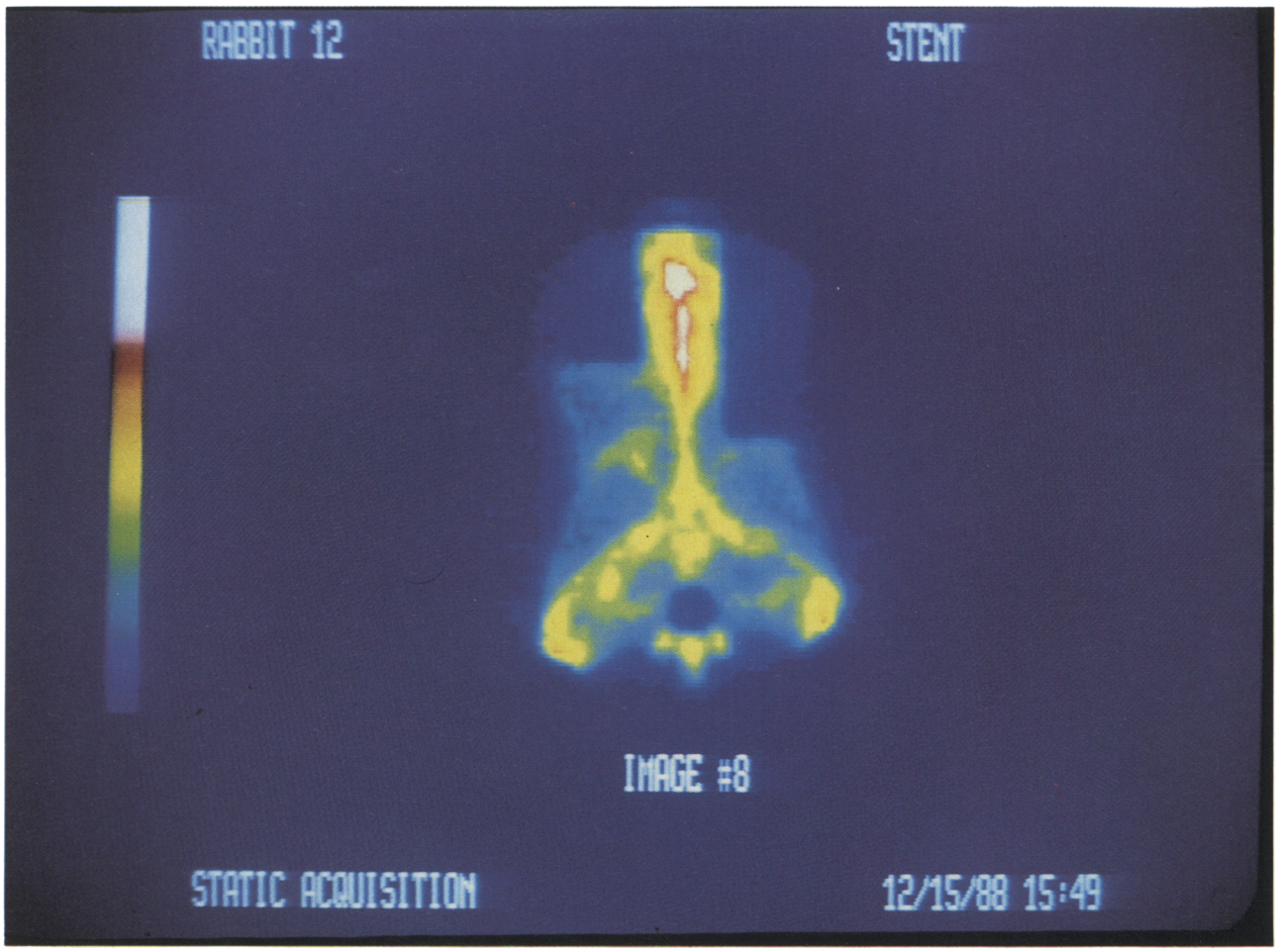

a probability value of less than 0.05 was required to reject the null hypothesis. All statistics were performed using commercially available software (RS-1, Bolt Baranek-Newman, Cambridge, Mass.).

Results

In Vivo Imaging Studies

Results of the in vivo S12 Fab′ monoclonal antibody imaging studies in all 43 rabbits are presented in Table 1 and Figure 2. There was no significant difference in the aortic arterial injury ratio between seven unfed and seven cholesterol-fed uninjured control rabbits (1.1±0.13 and 1.2±0.13, respectively; p=NS). Figure 3 illustrates in vivo and ex vivo imaging data for a cholesterol-fed control rabbit. One PTA (1.3±0.17) and two PTA procedures performed 6 weeks apart (1.4±0.22) significantly increased the acute injury ratio (p<0.05 versus unfed controls).

S12 activity ratios were quantitatively evaluated in the same ROIs used to calculate 60-minute values at 5 and 30 minutes after injection. Although unfed control group S12 activity ratio remained constant in the presence (5 and 30 minutes) and absence (60 minutes) of significant blood pool activity (1.09±0.07 to 1.08±0.02 to 1.09±0.13), a progressive increase in S12 activity ratio (1.19±0.09 to 1.35±0.21 to 1.57±0.28) occurred with blood pool clearance in PTA plus stent aortas. These data confirm the qualitative determination that S12 activity at injury sites was best evaluated at 60 minutes.

One week after PTA plus stent placement, the injury ratio had decreased significantly (1.1±0.10, p<0.05 versus acute PTA plus stent studies) to values not different from controls. Carotic TEC atherectomy in four heparinized rabbits did not acutely increase S12 antibody uptake in vivo (1.23±0.06), although one rabbit did exhibit increased ex vivo S12 activity (Figure 5).

Ex Vivo Imaging Studies

Arteries from 25 rabbits were excised immediately after completion of in vivo imaging for ex vivo imaging of S12 antibody distribution (Table 1). As with the in vivo images, there was no difference between the injury ratios in unfed and cholesterol-fed controls (1.0±0.11 versus 1.27±0.5, respectively; p=NS).

Ex vivo S12 activity was increased at single PTA sites (2.1±0.35, n=3, p<0.05 versus controls). PTA plus stent placement (Figure 4) significantly increased the ex vivo injury ratio (5.3±3.8, p<0.05 versus controls and one PTA study). The 1-week post–PTA and stent placement ex vivo injury ratio

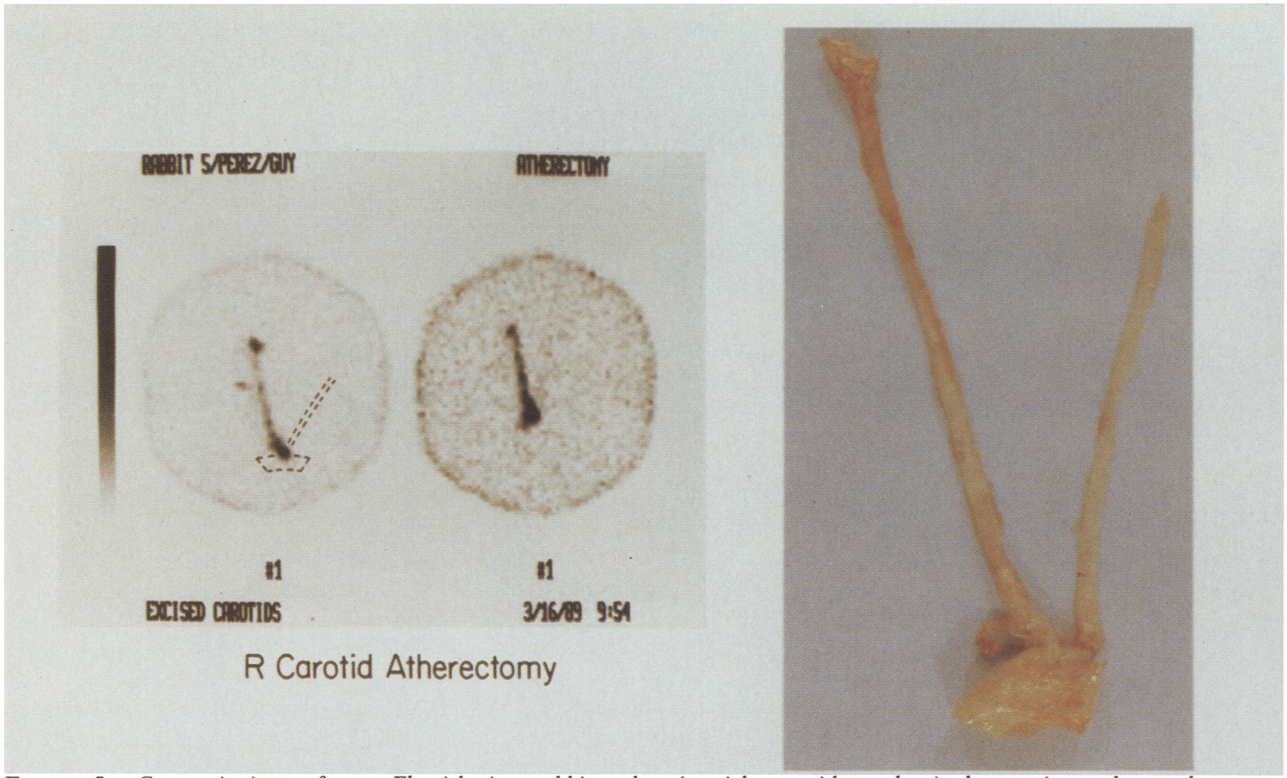

FIGURE 5. *Composite image from a Flemish giant rabbit undergoing right carotid transluminal extraction catheter atherectomy showing gross pathology* (right panel) *and ex vivo images of the excised carotids and aortic arch acquired 12 hours after injection of S12 monoclonal antibody. There is intense uptake throughout the length of the atherectomized right carotid artery (injury ratio, 1.2 in vivo and 7.0 ex vivo), with no uptake in the control carotid artery and aortic arch.*

decreased significantly (1.6±0.69, $p<0.05$ versus paired PTA plus stent data) to levels not different from those of controls.

Parallel studies with coinjection of a panel of ^{99m}Tc-labeled nonrelevant monoclonal antibodies to human macrophage (32.2) and breast cancer (C27) antigens ($n=3$ per group) revealed minimal nonspecific uptake in injured arterial segments compared with studies with S12. Human anti–macrophage antibody–specific activities in control and cholesterol-fed PTA aortas were 0.12±0.04 and 0.69±0.23 μCi/g aorta, respectively. Anti–breast cancer antibody–specific activity was 0.06±0.004 and 0.20±0.01 μCi/g in similar experimental groups. S-12–specific activities were 0.05±0.01 (p=NS versus 32.2 and C27) and 4.8±2.3 μCi/g ($p<0.01$ versus 32.2 and C27) in comparable studies.

Pathological Studies

Light microscopy. Light microscopy studies from rabbits selected from each group ($n=2$ per group) demonstrated significant increases in the intima-to-media ratio of cholesterol-fed balloon-injured rabbits compared with unfed controls (0.45±0.24 versus 0.08±0.03, $p<0.05$). Cholesterol feeding without prior arterial injury did not significantly increase the intima-to-media ratio (0.09±0.05, p=NS versus unfed controls). The atherosclerotic lesions induced were typical of this model[33] (Figure 1). Angiograms of these lesions before PTA and stent placement demonstrated diffuse irregularities with focal areas of aneurysmal dilatation in some animals.

Associated with acute PTA plus stent placement were marked endothelial cell loss; plaque fissuring and compression; extensive fibrin, red blood cells, white blood cells; platelet thrombus deposition (Figure 6); and no evidence of endothelial regeneration. Despite histological thrombus deposition at PTA and stent placement sties, all vascular lumens were grossly and angiographically patent.

Optical examination of the inner surface of aortas 1 week after stent placement revealed that all stents were covered by a translucent neointimal membrane (Figure 7), which was completely covered by endothelial cells with silver staining of cell borders (Figure 8A) that averaged 213±79 μm in thickness. The intima-to-media ratio increased to 1.9±0.92 ($p<0.05$ versus fed and unfed controls).

Scanning electron microscopy. Scanning electron microscopy of unfed and fed controls demonstrated essentially normal endothelial architecture. Single PTA injury caused extensive endothelial denudation and platelet deposition with polymorphic islands of residual normal endothelium. There was no evidence of medial disruption after PTA, possibly because of the fibrocellular nature of atherosclerotic plaques with minimal calcification in this rabbit model.

Stent struts remained essentially free of all cellular deposits acutely; however, interstices between the struts were extensively covered with fibrin strands,

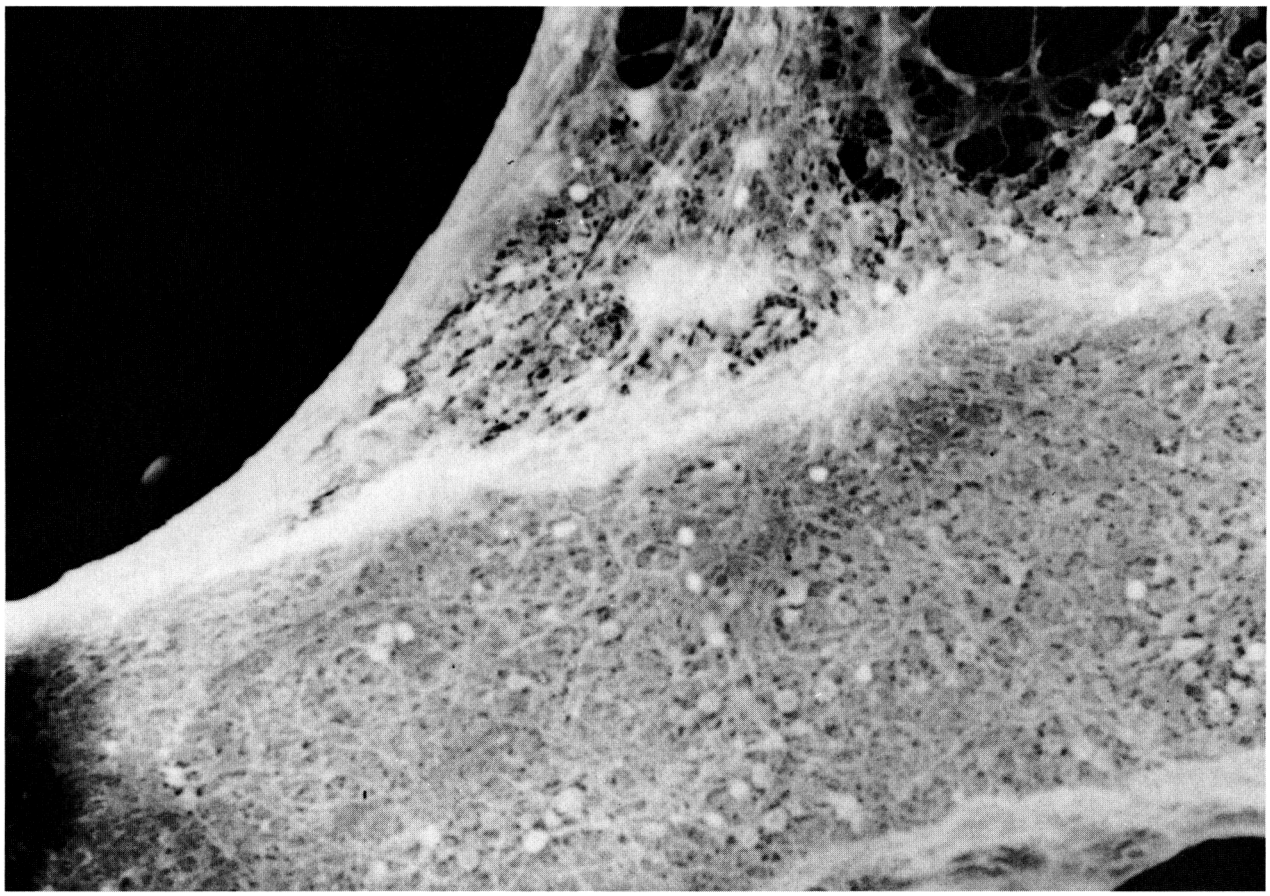

FIGURE 6. *Scanning electron microscopy (magnification, ×640) demonstrating extensive fibrin, red blood cell, and platelet deposition adherent to a stent strut after acute percutaneous transluminal angioplasty plus stent placement. The technetium-99m S12 injury ratio in this aorta was 1.5 in vivo and 2.5 ex vivo.*

white and red blood cells, and numerous platelets. One week after PTA plus stent placement, scanning electron microscopy revealed extensive neointima covered nearly completely by endothelial cells with borders outlined by silver deposits demonstrated by electron microscopy (Figure 8B). The new endothelial cells were immature, as evidenced by their prominent nuclei, polygonal cell shape, and mosaic growth pattern. There was a complete absence of platelets in the injury site.

Immunoelectron microscopy. Platelets reacted strongly with the monoclonal S12 antibody, with an average 22-fold increase in platelet labeling over the negative control IgG. Despite the partial deterioration of platelet structural integrity associated with preservation, labeling was predominantly localized to vacuoles in the platelets that represent the surface-connected canalicular system (Figure 9). Some labeling of the α-granules, while not consistent, was also noted.

Discussion

The present study confirms previous in vitro data showing the high specificity of monoclonal S12 Fab′ antibody binding to the α-granule membrane glycoprotein, GMP-140, expressed on the surface of individual platelets.[28] Our in vivo and ex vivo imaging data demonstrate that increasingly vigorous and repeated interventional injuries produce a commensurate increase in S12 binding despite angiographic vessel patency. Electron micrographs confirmed extensive acute platelet deposition at atherosclerotic endothelial injury sites in association with immunoelectron microscopic evidence of avid S12 binding to activated platelets. Active neointimal proliferation without platelet activation or significant S12 uptake was observed 1 week after interventional procedures. Despite obvious neointimal proliferation, smooth muscle proliferative changes were minimal at 1 week after PTA in this rabbit model but have been described in humans and pigs at later time after PTA injury.[25,37]

Previous Imaging Studies

Platelet imaging studies have been used to detect left ventricular thrombus formation,[24] in peripheral arteries after angioplasty,[22,23] and in coronary artery thrombi.[25] The presence of high nonspecific blood pool background activity due to circulating inactivated platelets has necessitated either dual-tracer subtraction techniques, which are sensitive to motion artifact, or reliance on delayed imaging studies of long half-life radioisotopes (e.g., indium-111 and

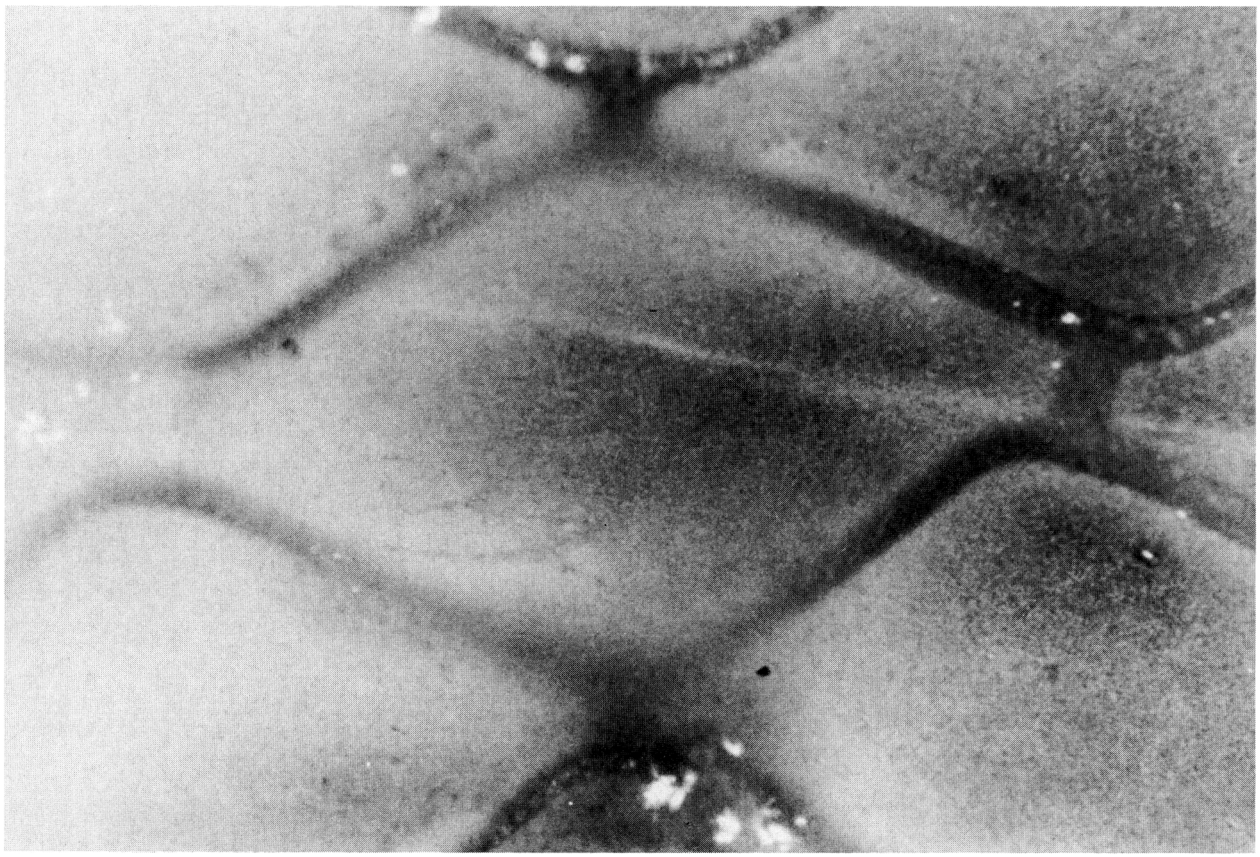

FIGURE 7. *Silver staining optical microscopy 1 week after percutaneous transluminal angioplasty plus stent placement reveals that stent struts are covered by a translucent coating of neointima.*

iodine-123) to permit thrombus visualization after clearance of blood pool activity.

The monoclonal antibodies 7E3 and P256, which are specific for platelet surface membrane glycoprotein IIb-IIIa, have been used for in vivo imaging of deep-vein thrombosis with ^{123}I-labeled 7E3[38] and canine vascular thrombus using ^{111}In-labeled P256 antibody.[39]

Another monoclonal antibody within this cluster of differentiation with specificity for translocated α-granule membrane protein of activated platelets, anti-PADGEM, has been labeled with ^{123}I for detection of deep venous thrombosis in a baboon model.[31] The imaging advantages identified in this study included low blood pool activity and rapid blood pool clearance (α t½, 2–6 minutes; β t½, 4 hours). In this model, venous thrombus was discernible at 15 minutes after injection, with 2-hour target-to-background ratios comparable to those in the present study (averaging 3:1 in vivo).

S12 monoclonal antibody exhibits high in vitro specificity (50:1) for thrombin-stimulated degranulating platelets.[27,28,40] Our immunoelectron microscopic studies of post-PTA thrombi confirmed the high in vivo specificity of S12 for activated platelet α-granule GMP-140 (22:1) compared with nonrelevant antibodies. Lower-level binding of S12 to vascular endothelial GMP-140 in the Weibel-Palade bodies containing von Willebrand factor[33] may have accounted for minimal binding of S12 Fab in atherosclerotic uninjured arterial segments.

Clinical Implications

The S12 monoclonal antibody used in the present study is reactive with human platelets. Phase I clinical trials are under way to evaluate S12 uptake in patients injected intravenously and imaged at 1, 4, and 24 hours after coronary and peripheral vessel angioplasty and amputation for severe arterial insufficiency. These preliminary studies indicate that the initial (4–6-hour) injury ratio and the duration of S12 image-derived platelet activity (less than 24 hours versus more than 24 hours) correlate with the presence of dissection and greater residual stenosis (i.e., turbulence) at PTA sites.[41]

The mean values in the unfed control group (1.09±0.13) and the cholesterol-fed control group (1.18±0.13) did not differ significantly from each other and did not equal 1.0 due to the presence of regionally variable secondary counts in the control aortas. For these control groups, the mean±1 SD values were 1.22 and 1.31, respectively. If the value of 1.3 is considered the upper limit of normal, this test would have an 86% specificity and sensitivity in the control, PTA twice, and PTA plus stent subgroups. Using a 2 SD above the control group mean (1.4) as the upper limit of normality, four of seven (57%) of the PTA twice and five of

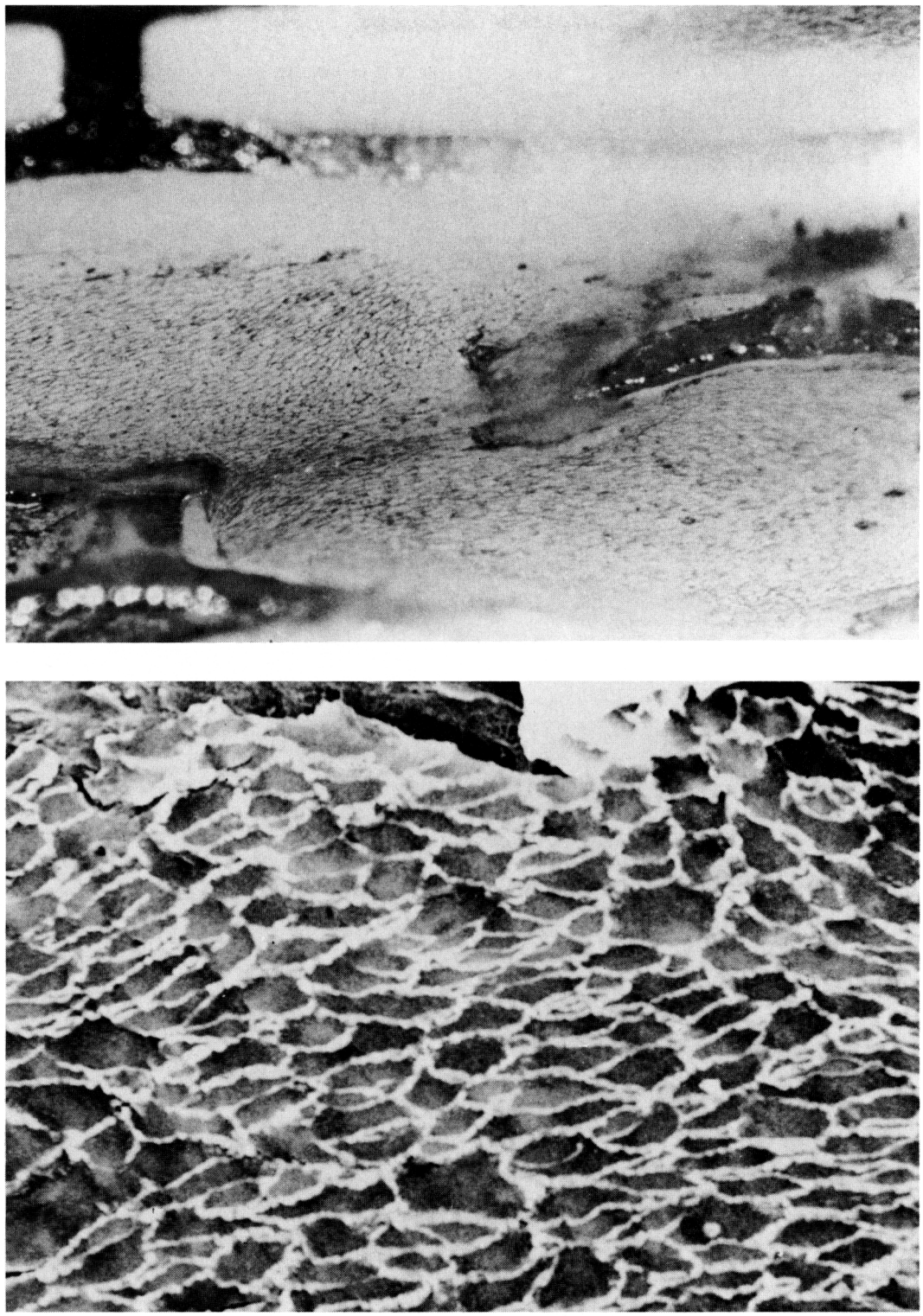

FIGURE 8. Top panel: *Optical microscopic examination of neointimal formation overlying a stent strut 1 week after placement demonstrating silver deposits outlining the borders of endothelial cells and a mosaic pattern characteristic of endothelial cell regrowth.* Bottom panel: *Higher magnification electron microscopy (magnification, ×640) from the same rabbit aorta further demonstrating the mosaic pattern of endothelial regrowth surrounding an islet of persistent endothelial denudation 1 week after stent placement, with prominent nuclei and polygonal shape of the immature endothelial cells. Relative absence of platelets and cellular elements from the 1 week poststent specimens was correlated with a reduced S12 antibody injury ratio of 1.12 in vivo and 1.25 ex vivo in this experiment.*

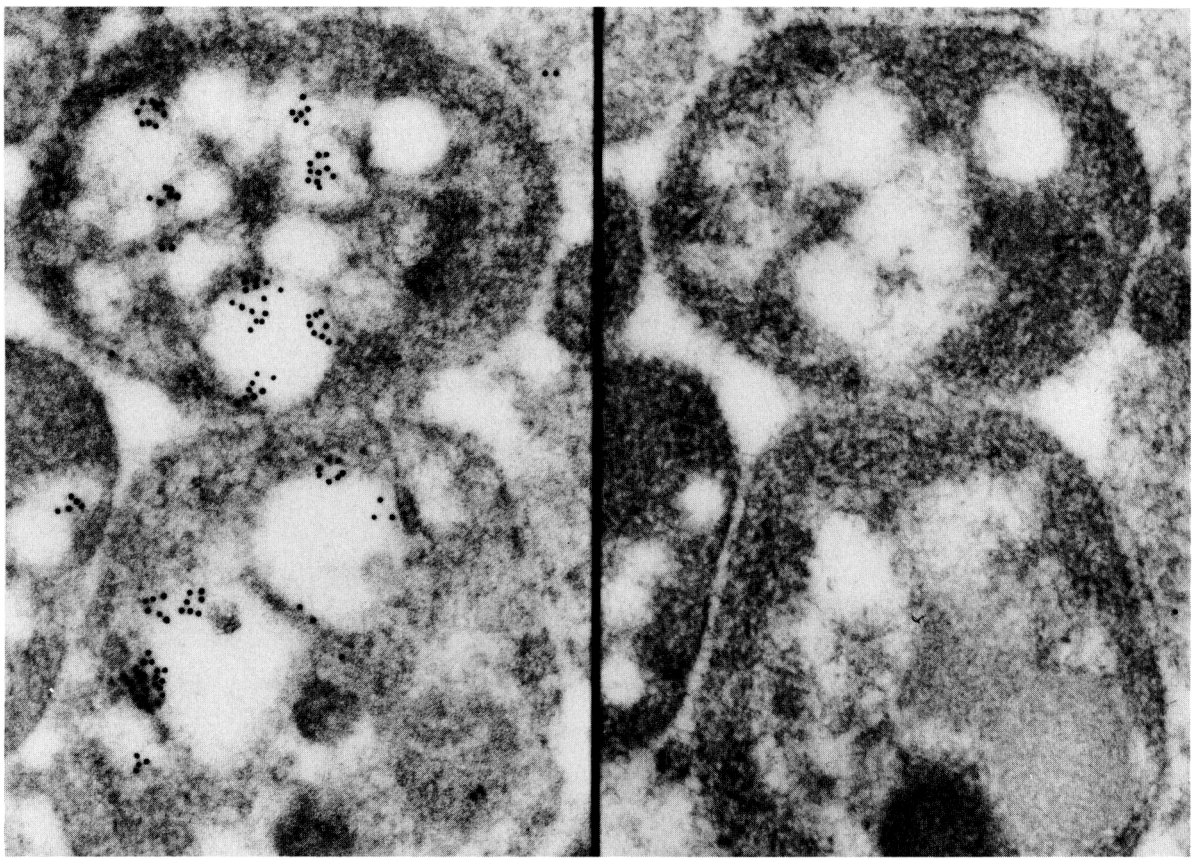

FIGURE 9. *Immunoelectron microscopic study of platelets extracted from an angioplasty injury site reacted with S12 monoclonal antibody* (left panel) *and nonrelevant antibody* (right panel). *There is predominant S12 labeling with electron-dense colloidal gold particles at the vacuolated regions of the activated platelets, representing the platelet surface–connected canalicular system expression of GMP-140 originating in the α-granules* (bottom). *A negative control using the mouse preimmunized sera showing the same platelets sectioned at a different level without any significant labeling (magnification, ×61,000). Minimal amounts of extracellular labeling represents membraneous platelet debris included in the clot.*

seven (71%) of the PTA plus stent studies exceeded this cutoff, for an overall sensitivity of 64% and specificity of 93% in these four groups ($n=28$). The separation between "normal" and elevated S12 activity ratios in vivo provides diagnostic accuracy that is comparable to that of other antibody-imaging techniques, with acceptable specificity. High initial blood pool activity and individual variability of tracer uptake at injury sites have also been encountered in preliminary clinical studies with this agent.

In our acute in vivo animal studies, platelet-rich thrombi were detected in stents with expanded dimensions of 3×5 mm using a standard planar gamma camera. The greater S12 injury ratios observed in excised aortas demonstrate that removal of free ^{99m}Tc by manual blood pool subtraction improved localization of S12 uptake compared with 1-hour in vivo images. Based on preliminary clinical studies[41] showing clearance of blood pool activity by 4–6 hours after S12 injection and animal studies that demonstrate that only 6±2% of the originally injected dose per gram of blood remains at 6 hours after injection,[42] the calculated (decay-corrected) percent of injection dose available in blood is 17% at 6 hours. Incorporation of the ^{99m}Tc label onto S12 Fab′ averages 96% at 1 hour of incubation time, after which the labeling efficiency (in human plasma at 37°C) averages 89% at 24 hours (data on file, Centocor, Inc., Malvern, Pa.). Variability in S12 uptake in unheparinized subgroups or rabbits under carefully controlled experimental conditions and heparinized patients after PTA[41] suggests that individual characteristics may also influence S12 binding.

Cyclooxygenase inhibitors that are effective in acute thrombosis do not effectively block platelet α-granule secretion[43] and do not prevent restenosis after angioplasty.[15] Clinicopathological and experimental studies clearly implicate exuberant neointimal smooth muscle proliferation mediated by local platelet-derived growth factor release as the etiology of post-PTA restenosis.[7,17–19,21] The cellular event detected by these S12 studies is platelet activation and secretion of stored α-granule proteins, including growth factors,[27,28] a process distinct from that causing acute vessel closure.[7]

The clinical usefulness of in vivo ^{99m}Tc S12 imaging for localization of interventional injury sites is implied but remains unproven. S12 Fab′ imaging may

assist in the prospective evaluation of PTA and other interventional therapies by identifying patients with greater acute platelet degranulization and local growth factor release who are at higher risk of restenosis and in need of more aggressive pharmacotherapy and angiographic follow-up.

Acknowledgments

The authors wish to acknowledge the expert technical assistance of Betty W. Heyl and Lisa Stumpoand and the secretarial efforts of Debbie Brown and Lynda Larsen. Also, we appreciate the preparation of S12 by Dr. Tuhin K. Chandhuri, MD, and Mr. John Straw (Division of Nuclear Medicine, Audie Murphy Veterans Administration Hospital, San Antonio, Tex.).

References

1. Fitzgerald DJ, Roy L, Catella FG, Fitzgerald GA: Platelet activation in unstable coronary disease. *N Engl J Med* 1986; 315:983–989
2. Fuster V, Chesebro JH: Mechanics of unstable angina. *N Engl J Med* 1986;315:1023–1025
3. Hirsh PD, Hillis LD, Campbell WB, Firth BG, Willerson JT: Release of prostaglandins and thromboxane A_2 into the coronary circulation in patients with ischemic heart disease. *N Engl J Med* 1981;304:685–691
4. Folts JD, Crowell EB, Rowe GG: Platelet aggregation in partially obstructed vessels and its elimination with aspirin. *Circulation* 1976;54:365–370
5. Lewis HD, David JW, Archibald DG, et al: Protective effects of aspirin against acute myocardial infarction and death in men with unstable angina: Results of a Veterans Administration cooperative study. *N Engl J Med* 1983;309:396–403
6. Cairns JA, Gent M, Singer J, et al: Aspirin, sulfinpyrazone, or both in unstable angina: Results of a Canadian multicenter trial. *N Engl J Med* 1985;313:1369–1375
7. Fuster V, Adams PC, Badimon JJ, Chesebro JH: Platelet-inhibitor drugs' role in coronary artery disease. *Prog Cardiovasc Dis* 1987;29:325–346
8. Diodati J, Theroux P, Latour JG, Roy D, Waters DD: Nitroglycerin at therapeutic doses inhibits platelet aggregation in man. *J Am Coll Cardiol* 1988;11(2):54A
9. Holmes DR Jr, Vliestra RE, Smith HC, et al: Restenosis after PTCA: A report from the PTCA registry of the National Heart, Lung, and Blood Institute. *Am J Cardiol* 1984;53:77C–81C
10. Jutzy KR, Berte LE, Alderman EL, et al: Coronary restenosis rates in consecutive patient series one year post-successful angioplasty. *Circulation* 1982;66(suppl II):II-331
11. Hollman J, Gruentzig AR, Meier B, et al: Factors affecting recurrence after successful coronary angioplasty. *J Am Coll Cardiol* 1983;1:1644
12. Hollman J, Austin GE, Gruentzig AR, et al: Coronary artery spasm at the site of angioplasty in the first 2 months after successful percutaneous transluminal coronary angioplasty. *J Am Coll Cardiol* 1983;2:1039–1045
13. Whitworth HB, Roubin GS, Hollman J, et al: Effects of nifedipine on recurrent stenosis after PTCA. *J Am Coll Cardiol* 1986;8:1271–1276
14. Corcos T, David PR, Val PG, et al: Failure of diltiazem to prevent restenosis after PTCA. *Am Heart J* 1985;109:926–931
15. Schwartz L, Bourassa MG, Lesperance J, et al: Aspirin and dipyridamole in the prevention of restenosis after percutaneous transluminal coronary angioplasty. *N Engl J Med* 1987;318: 1714–1719
16. Ross R, Glomset J, Kariya B, et al: A platelet dependent serum factor that stimulates proliferation of arterial smooth muscle cells in vitro. *Proc Natl Acad Sci USA* 1974;71:1207–1210
17. Austin GE, Ratliff NB, Hollman J, et al: Intimal proliferation of smooth muscle cells as an explanation for recurrent coronary artery stenosis after percutaneous transluminal coronary angioplasty. *J Am Coll Cardiol* 1985;6:369–375
18. Kohchi K, Takebayashi S, Block PC, et al: Arterial changes after PTCA: Results at autopsy. *J Am Coll Cardiol* 1987;10:592–599
19. Steele PM, Chesebro JH, Stanson AW, et al: Balloon angioplasty: Natural history of the pathophysiologic response to injury in a pig model. *Circ Res* 1985;57:105–112
20. Lam JYT, Chesebro JH, Fuster V: Is arterial vasospasm during angioplasty in pigs related to platelet deposition, arterial injury, or both? *Circulation* 1985;72(suppl III):III-218
21. Waller BF: Crackers, breakers, stretchers, drillers, scrapers, shavers, burners, welders, and melters—The future treatment of atherosclerotic coronary artery disease? A clinical-morphologic assessment. *J Am Coll Cardiol* 1989;13:969–987
22. Lam JYT, Chesebro JH Steele PM, et al: Deep arterial injury during experimental angioplasty: Relation to a positive indium-III labeled platelet scintigram, quantitative platelet deposition and mural thrombosis. *J Am Coll Cardiol* 1986;8: 1380–1386
23. Ezekowitz MD, Pope CF, Smith EO, et al: Indium-III platelet deposition at sites of percutaneous transluminal peripheral angioplasty. *Circulation* 1982;68(suppl III):III-144
24. Ezekowitz MD, Leonard JC, Smith EO, et al: Identification of left ventricular thrombi in man using indium-III labeled autologous platelets. *Circulation* 1981;63:803
25. Bergmann SR, Lerch RA, Mathias CJ, et al: Noninvasive detection of coronary thrombi with indium-III platelets: Concise communication. *J Nucl Med* 1983;24:130–135
26. Oster ZH, Srivastava SC, Som P, Meinken GE, Scudder LE, Yamamoto K, Atkins HL, Brill AB, Coller BS: Thrombus radioimmunoscintigraphy: An approach using monoclonal antiplatelet antibody. *Proc Natl Acad Sci USA* 1985;82: 3465–3468
27. Stenberg PE, McEver RP, Shuman MA, et al: A platelet alpha-granule membrane protein (GMP-140) is expressed on the plasma membrane after activation. *J Cell Biol* 1985;101: 880–886
28. McEver RP, Martin MN: A monoclonal antibody to a membrane glycoprotein binds only to activated platelets. *J Biol Chem* 1984;259:9799–9804
29. Berman CL, Yeo EL, Wencel-Drake JD, Furie BC, Ginsberg MH, Furie B: A platelet alpha granule membrane protein that is associated with the plasma membrane after activation. *J Clin Invest* 1986;78:130–137
30. Hsu-Lin SC, Berman CLK, Furie BC, August D, Furie B: A platelet membrane protein expressed during platelet activation and secretion: Studies using a monoclonal antibody specific for thrombin-activated platelets. *J Biol Chem* 1984;259: 9121–9126
31. Palabrica TM, Furie BC, Konstam MA, Aronovitz MJ, Connolly R, Brockway BA, Ramber KL, Furie B: Thrombus imaging in a primate model with antibodies specific for an external membrane protein of activated platelets. *Proc Natl Acad Sci USA* 1989;86:1036–1040
32. Palmaz JC, Windeler SA, Garcia F, et al: Atherosclerotic rabbit aortas: Expandable intraluminal grafting. *Radiology* 1986;160:723–726
33. Baumgartner HR: Eine neue method zur erzeugung von thromben durch zielte uberdehnung der gefasswand. *Ges Exp Med* 1963;173:227–247
34. Shimokawa H, Tomoike H, Nabeyama S, et al: Coronary artery spasm induced in atherosclerotic miniature swine. *Science* 1983;221:560–562
35. Heistad DD, Armstrong ML, Marcus ML, et al: Augmented responses to vasoconstrictor stimuli in hypercholesterolemic and atherosclerotic monkeys. *Circ Res* 1984;54:711–718
36. Pak KY, Dean R, Mattis J, Khaw BA, Powers J, Kanke M, Berger H: Tc-99m antimyosin infarct-avid scintigraphy: Improved results with a new instant kit labeling technique suitable for routine use. *Circulation* 1987;76(suppl IV):IV-2013
37. Lam JYT, Chesebro JH, Heras M, et al: Deep and superficial arterial injury: Different affinity for thrombus formation at increasing shear rate. *Circulation* 1987;76(suppl IV):IV-101

38. Stuttle AWJ, O'Donnell CJ, Virji N, et al: Imaging thrombus with radiolabelled Fab' fragments of a monoclonal antibody to platelets. *J Nucl Med* 1988;29:940
39. Coller BS, Oster ZH, Meinken GE, et al: Autologous dog platelets (P) reacted with an 111-indium-labeled monoclonal antibody to GPIIb/IIIa can be used to image thrombi. *Circulation* 1984;70(suppl II):II-195
40. McEver RP, Beckstead JH, Moore KL, Marshall-Carlson L, Bainton DF: GMP-140, a platelet α-granule membrane protein, is also synthesized by vascular endothelial cells and is localized in Weibel-Palade bodies. *J Clin Invest* 1989;84:92–99
41. Miller DD, Palmaz JC, Garcia OJ, et al: Platelet activation at human angioplasty sites: Noninvasive detection by specific S12 monoclonal antibody imaging. *Circulation* 1990;82(suppl III): III-650
42. Nedelman MA, Boulet AJ, Miller DD, Neblock DS, Pak KY, Berger HJ: In vivo imaging of acute arterial thrombi with technetium-99m anti-platelet monoclonal antibody. *J Am Coll Cardiol* 1990;15:170A
43. Shattil SJ, Bennett JS: Platelets and their membranes in hemostasis: Physiology and pathophysiology. *Ann Intern Med* 1980;94:108–118

KEY WORDS • monoclonal antibodies • platelets • radionuclide imaging • percutaneous transluminal angioplasty • atherosclerosis